

# Tea polyphenol protects against cisplatin-induced meiotic defects in porcine oocytes

Changyin Zhou<sup>1</sup>, Xue Zhang<sup>1</sup>, Xiayan ShiYang<sup>1</sup>, Huili Wang<sup>2</sup>, Bo Xiong<sup>1</sup>

<sup>1</sup>College of Animal Science and Technology, Nanjing Agricultural University, Nanjing 210095, China

<sup>2</sup>Institute of Animal Science, Jiangsu Academy of Agricultural Sciences, Nanjing 210014, China

**Correspondence to:** Bo Xiong; email: [xiongbo@njau.edu.cn](mailto:xiongbo@njau.edu.cn)

**Keywords:** cisplatin, tea polyphenol, oocyte quality, meiotic failure, organelle dynamics

**Received:** April 18, 2019

**Accepted:** July 1, 2019

**Published:** July 13, 2019

**Copyright:** Zhou et al. This is an open-access article distributed under the terms of the Creative Commons Attribution License (CC BY 3.0), which permits unrestricted use, distribution, and reproduction in any medium, provided the original author and source are credited.

## ABSTRACT

**DDP (cisplatin), a DNA cross-linking agent, is one of the most common chemotherapeutic drugs that have been widely used in the treatment of sarcomas and germ cell tumors. DDP treatment exhibits severe side effects including renal toxicity, ototoxicity and embryo-toxicity. Women of reproductive age treated with DDP may lead to loss of primordial follicles, resulting in the depletion of the ovarian reserve and consequent premature ovarian failure. However, the influence of DDP on the oocyte quality and the strategy to prevent it has not yet fully clarified. Here, we report that DDP exposure resulted in the oocyte meiotic failure via disrupting the meiotic organelle dynamics and arrangement, exhibiting a prominently impaired cytoskeleton assembly, including spindle formation and actin polymerization. In addition, exposure to DDP led to the abnormal distribution of mitochondrion and cortical granules, two indicators of cytoplasmic maturation of oocytes. Conversely, TP (tea polyphenols) supplementation partially restored all of the meiotic defects resulted from DDP exposure through suppressing the increase of ROS level and the occurrence of DNA damage as well as apoptosis.**

## INTRODUCTION

Cisplatin (DDP) was first described by Michele Peyrone in 1845, and its structure was determined in 1893 [1, 2]. After a long time of investigation, Rosenberg found its potential role in inducing the death of tumor cells and finally in 1978 it was approved by the FDA as a drug for the treatment of testicular and ovarian cancer [2]. Nowadays, DDP has been widely applied to treat a couple of tumors, such as ovary, testes, gastric, head and neck, non-small cell lung, gallbladder and urinary bladder [3–5]. DDP is an alkylating agent capable of forming adducts with macromolecules, particularly with N7 atoms of purine nucleobases, which results in inter- and intra-strand DNA cross-links [6, 7]. The inability to repair the DNA damage ultimately leads to the programmed cell death [8]. In addition, experimental evidence has revealed that other mechanisms, such as the production of reactive oxygen species (ROS) and

the activation of inflammatory pathways, may also contribute to the DDP-induced apoptosis [9].

Nevertheless, DDP treatment displays a variety of side effects including immunosuppression, renal toxicity, gastrointestinal disorders and ototoxicity [10]. It also causes gonadal suppression resulting in amenorrhea or azoospermia, partial or irreversible infertility and embryo-toxicity [11]. Additionally, as a first-line agent for ovarian cancer treatment [5, 12], DDP-induced gonadotoxicity leads to the changes in the menstrual cycle and loss of primordial follicles by apoptosis, resulting in the depletion of the ovarian reserve and consequent premature ovarian failure [13, 14]. However, the molecular mechanisms regarding how DDP influences the oocyte quality has not yet determined.

Tea, a popular beverage consumed world-wide, has been studied for its preventive effects against cancer as well as

cardiovascular, neurodegenerative, and other diseases [15]. Most of the proposed beneficial effects in tea have been attributed to the polyphenolic compounds. TP (tea polyphenol) is known to be a strong antioxidant that can prevent the oxidative stress and DNA damage to modulate the carcinogen metabolism in many cell lines and animal models [15–20]. Furthermore, it has been reported that TP protects spermatogenesis against ionizing radiation-induced testicular injury in mice [21], improves the follicular development in rats, and promotes oocyte maturation as well as embryo development in bovines [22–25].

In current study, we used porcine oocytes as a research model to investigate the effects of DDP exposure on the oocyte quality because porcine oocytes and human oocytes have developmental and physiological similarities [26, 27]. We find that DDP exposure results in the meiotic failure in porcine oocytes through compromising the cytoskeleton organization, mitochondrial integrity and cortical granule distribution. Conversely, TP effectively suppresses the increased oxidative stress-induced DNA damage and apoptosis, thereby restoring the meiotic failure induced by DDP in oocytes.

## RESULTS

### TP alleviates the meiotic failure of oocytes exposed to DDP

To examine the effects of DDP exposure on porcine oocyte meiotic maturation, different concentrations of DDP were supplemented to IVM medium (2, 5, 10 or 20  $\mu\text{M}$ ). After culturing for 44 h *in vitro*, we observed the developmental status of COCs and the proportion of polar body extrusion (PBE). As shown in Figure 1A, most of the cumulus cells surrounding COCs in the control group were fully expanded, while those in the DDP-exposed group were only partially expanded or not expanded (Figure 1A). Moreover, a majority of oocytes extruded the first polar body in the control group, but failed to do so after DDP treatment (Figure 1A). Quantitative data revealed that the proportion of PBE was reduced in a dose-dependent manner after DDP treatment compared with the controls (control:  $69.2 \pm 2.2\%$ ,  $n=149$ ; 2  $\mu\text{M}$  DDP:  $65.2 \pm 2.0\%$ ,  $n=144$ ,  $P > 0.05$ ; 5  $\mu\text{M}$  DDP:  $55.9 \pm 2.4\%$ ,  $n=139$ ,  $P < 0.05$ ; 10  $\mu\text{M}$  DDP:  $35.1 \pm 2.3\%$ ,  $n=149$ ,  $P < 0.001$ ; 20  $\mu\text{M}$  DDP:  $12.3 \pm 2.2\%$ ,  $n=146$ ,  $P < 0.001$ ; Figure 1B). We selected the concentration of 10  $\mu\text{M}$  DDP for further studies because it allowed a portion of oocytes to be matured for other studies.

To ask whether supplementation of TP would have beneficial impact on the meiotic defects caused by the

DDP exposure, different concentrations of TP (10  $\mu\text{M}$ , 50  $\mu\text{M}$  and 250  $\mu\text{M}$ ) were supplemented into the maturation medium containing 10  $\mu\text{M}$  DDP. The results showed that supplementation of 50  $\mu\text{M}$  TP had the best improvement on the expansion of cumulus cells surrounding COCs and significantly increased the percentage of PBE compared with the DDP-exposed group ( $57.8 \pm 3.4\%$ ,  $n=144$  VS  $34.5 \pm 1.9\%$ ,  $n=140$ ,  $P < 0.01$ ; Figure 1A, 1C). Taken together, these observations suggest that the defects of porcine oocyte maturation induced by DDP exposure could be, at least partially, restored by the supplementation of TP.

### TP recovers the defects of spindle/chromosome structure in DDP-exposed oocytes

Given that the arrest of oocyte meiotic progression is usually linked with the impairment of cytoskeleton structures [28, 29], we confirmed this possibility by staining the spindle structure and chromosome alignment in DDP-exposed oocytes. In control oocytes a standard barrel-shape spindle structure with a well-aligned chromosome on the equatorial plate was exhibited (Figure 2A). By contrast, a higher frequency of aberrant spindle morphologies with misaligned chromosomes was present in DDP-exposed oocytes (spindle:  $15.0 \pm 1.8\%$ ,  $n=114$  VS  $43.8 \pm 5.1\%$ ,  $n=124$ ,  $P < 0.01$ ; chromosome:  $17.5 \pm 1.1\%$ ,  $n=109$  VS  $44.9 \pm 2.8\%$ ,  $n=122$ ,  $P < 0.001$ ; Figure 2A–2C). Conversely, supplementation of TP in the DDP-exposed group substantially reduced the incidence of abnormal spindle/chromosome structure (spindle:  $24.5 \pm 1.2\%$ ,  $n=106$ ,  $P < 0.05$ ; chromosome:  $30.1 \pm 1.3\%$ ,  $n=120$ ,  $P < 0.01$ ; Figure 2A–2C).

### TP maintains the acetylation level of $\alpha$ -tubulin in oocytes exposed to DDP

Studies have shown that the disorganized spindle structure might be resulted from the disruption of acetylation level of  $\alpha$ -tubulin, an indicator of stable microtubules in oocytes [30–33]. Therefore, we next assessed the level of acetylated  $\alpha$ -tubulin in oocytes exposed to DDP. Immunostaining analysis and quantitative measurement of the fluorescence intensity indicated that  $\alpha$ -tubulin in DDP-exposed oocytes displayed an apparently decreased level of acetylation compared with the controls ( $16.0 \pm 2.1$ ,  $n=52$  VS  $45.4 \pm 2.6$ ,  $n=55$ ,  $P < 0.001$ ; Figure 3A, 3B). While TP supplementation remarkably raised the signals of acetylated  $\alpha$ -tubulin in DDP-exposed oocytes ( $38.3 \pm 2.0$ ,  $n=57$  VS  $16.0 \pm 2.1$ ,  $n=52$ ,  $P < 0.01$ ). These observations were further confirmed by the immunoblotting analysis (Figure 3C), implying that the recovery of perturbed spindle structure in DDP-exposed oocytes by TP supplementation might be mediated by the maintenance of acetylation level of  $\alpha$ -tubulin.

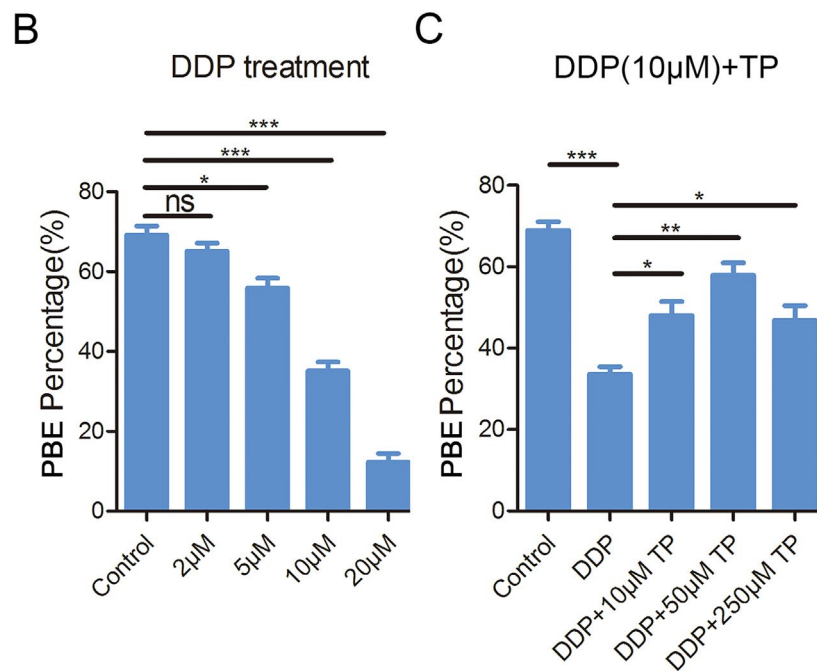
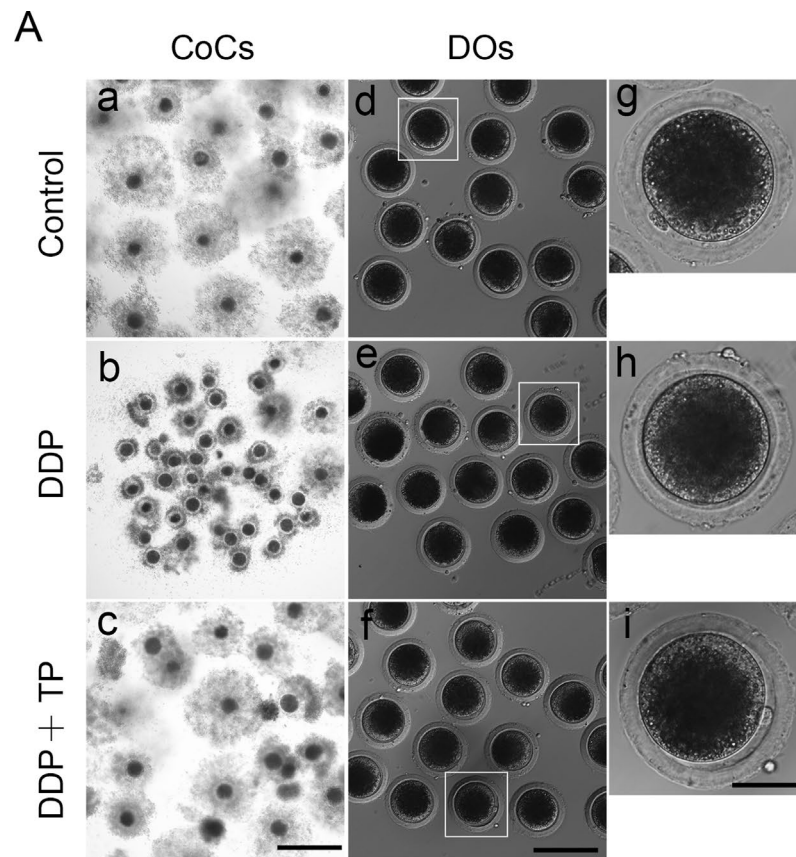


**Figure 1. Effects of different concentrations of DDP and TP on the porcine oocyte maturation.** (A) Representative images of oocyte meiotic progression in control, DDP -exposed and TP-supplemented oocytes. Cumulus cell expansion of COCs and polar body extrusion of DOs were imaged by the confocal microscope. Scale bar, 350  $\mu$ m (a-c); 120  $\mu$ m (d-f); 50  $\mu$ m (g-i). (B) The rates of polar body extrusion were recorded in control and different concentrations of DDP-exposed groups (2  $\mu$ M, 5  $\mu$ M, 10  $\mu$ M and 20  $\mu$ M) after culture for 44 h *in vitro*. (C) The rates of polar body extrusion were recorded in control and different concentrations of TP -supplemented groups (10  $\mu$ M, 50  $\mu$ M and 250 $\mu$ M) after culture for 44 h with 10  $\mu$ M DDP *in vitro*. Data in were presented as mean percentage (mean  $\pm$  SEM) of at least three independent experiments. \*P < 0.05, \*\*P < 0.01, \*\*\*P < 0.001.

## TP restores the polymerization of actin filaments in DDP-exposed oocytes

During oocyte meiotic maturation, the actin assembly plays a critical role in asymmetric spindle positioning and cortical polarization [34–36]. To investigate whether the meiotic defects induced by DDP exposure involves the actin dynamics, phalloidin-TRITC was employed to stain the F-actin to observe the polymerization of actin filaments. As shown in Figure 4A, actin filaments were concentrated uniformly on the plasma membrane with robust signals in control oocytes. By contrast, DDP-exposed oocytes displayed

the impaired assembly of actin filaments with weak signals (Figure 4A), which was confirmed by the fluorescence plot profiling that was quantified along the lines drawn through the oocytes (Figure 4B). In addition, the quantitative measurement of fluorescence intensity on the membrane revealed that actin signals were substantially decreased in DDP-exposed oocytes, but increased to the control comparable level after supplementation with TP (control:  $24.4 \pm 2.2$ ,  $n=47$ ,  $P < 0.01$ ; DDP:  $12.3 \pm 1.1$ ,  $n=49$ ; TP:  $22.3 \pm 1.2$ ,  $n=53$ ,  $P < 0.01$ ; Figure 4C), indicating that TP prevents the assembly of actin cytoskeleton from damage induced by DDP exposure.

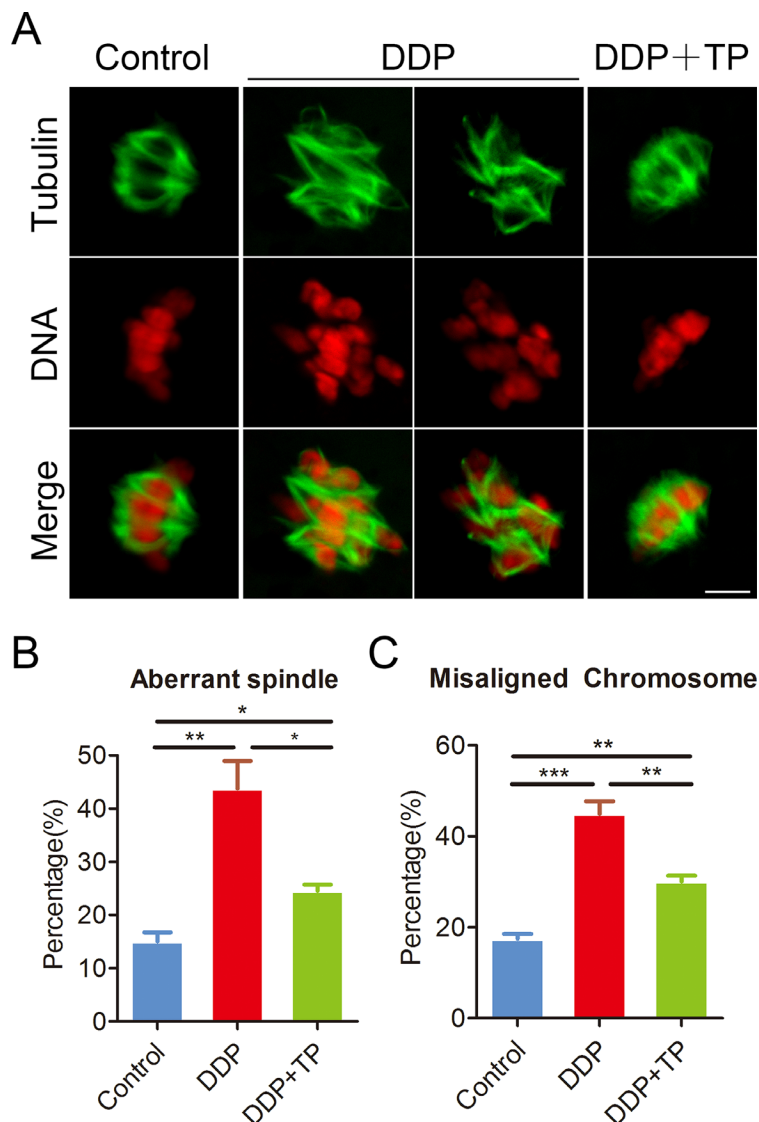


**Figure 2. Effects of TP on the spindle/chromosome defects in DDP-exposed porcine oocytes.** (A) Representative images of spindle morphologies and chromosome alignment in control, DDP-exposed and TP-supplemented oocytes. Scale bar, 5  $\mu$ m. (B) The rate of aberrant spindles was recorded in control, DDP-exposed and TP-supplemented oocytes. (C) The rate of misaligned chromosomes was recorded in control, DDP-exposed and TP-supplemented oocytes. Data in were presented as mean percentage (mean  $\pm$  SEM) of at least three independent experiments. \* $P < 0.05$ , \*\* $P < 0.01$ , \*\*\* $P < 0.001$ .

**TP rescues the distribution of CGs and mitochondria in DDP-exposed oocytes**

The distribution of CGs (cortical granules) and mitochondria are two key indexes of cytoplasmic maturation of oocytes [37, 38]. CGs are triggered at fertilization to migrate to the plasma membrane of oocytes, where they fuse and exocytose their contents to prevent polyspermy [39]. The results from Figure 5A

showed that the signals of CGs exhibited markedly faded following culture with DDP. The quantification analysis also confirmed that the fluorescence intensity of the signals had a significant decline in DDP-exposed oocytes compared to the controls ( $11.7 \pm 0.9$ ,  $n=52$  VS  $25.1 \pm 1.2$ ,  $n=51$ ,  $P < 0.001$ ; Figure 5B), and this decline was rescued by the supplementation of TP during *in vitro* culture ( $19.9 \pm 1.5$ ,  $n=47$ ,  $P < 0.01$ ; Figure 5B).

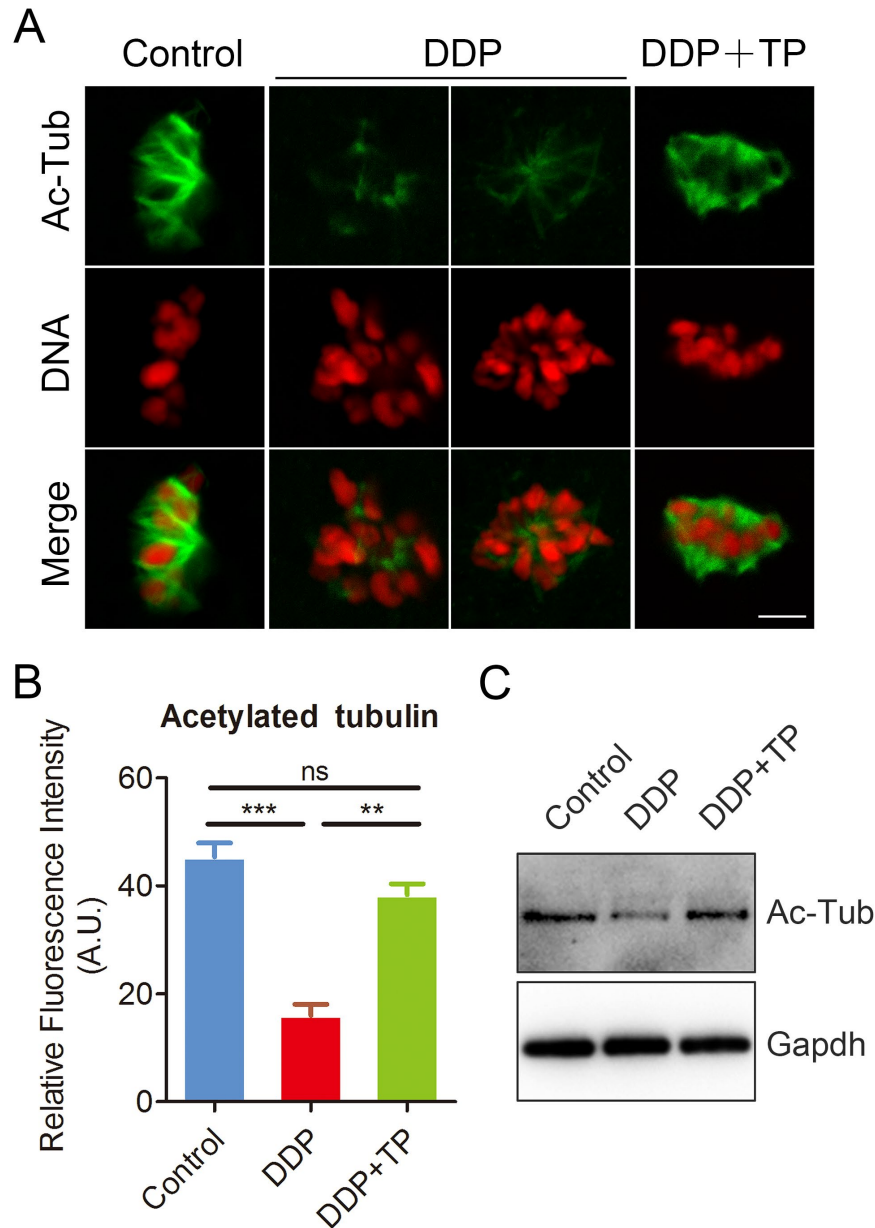


**Figure 3. Effects of TP on the acetylation level of  $\alpha$ -tubulin in DDP-exposed porcine oocytes.** (A) Representative images of acetylated  $\alpha$ -tubulin in control, DDP-exposed and TP-supplemented oocytes. Scale bar, 5  $\mu$ m. (B) Quantitative analysis of the fluorescence intensity of acetylated  $\alpha$ -tubulin in control, DDP-exposed and TP-supplemented oocytes. (C) The acetylation levels of  $\alpha$ -tubulin were detected by Immunoblotting in control, DDP-exposed and TP-supplemented oocytes. The blots were probed with anti-acetyl- $\alpha$ -tubulin and anti-Gapdh antibodies, respectively. Data were presented as mean percentage (mean  $\pm$  SEM) of at least three independent experiments. \*\*P < 0.01, \*\*\*P < 0.001.

In normal porcine oocytes most of mitochondria accumulated around lipid droplets in the subcortical region, but lost the specific localization in DDP-exposed oocytes (Figure 5C). The measurement of fluorescence intensity showed that signals of mitochondria prominently reduced in the DDP-exposed oocytes in comparison with the controls ( $22.6 \pm 1.5$ ,  $n=58$  VS  $45.1 \pm 1.8$ ,  $n=55$ ,  $P < 0.001$ ; Figure 5C, 5D). Conversely, this defect prevented by the treatment with TP ( $39.3 \pm 1.2$ ,  $n=49$ ,  $P < 0.001$ ; Figure 5C, 5D). We also assessed the mitochondrial membrane potential ( $\Delta\Psi_m$ ) by JC-1 staining.

Mitochondria with high membrane potential showed a red fluorescence while those with low membrane potential showed a green fluorescence (Figure 5E). The quantitative analysis revealed that the ratio of red and green fluorescence was significantly higher in control oocytes than that in DDP-exposed oocytes, but rescued in TP-supplemented oocytes ( $1.8 \pm 0.07$ ,  $n=27$ ,  $P < 0.001$  VS  $0.4 \pm 0.07$ ,  $n=28$  VS  $1.3 \pm 0.09$ ,  $n=27$ ,  $P < 0.01$ ; Figure 5F). Altogether, these observations indicate that TP restores the impairment of cytoplasmic maturation of oocytes exposed to DDP.

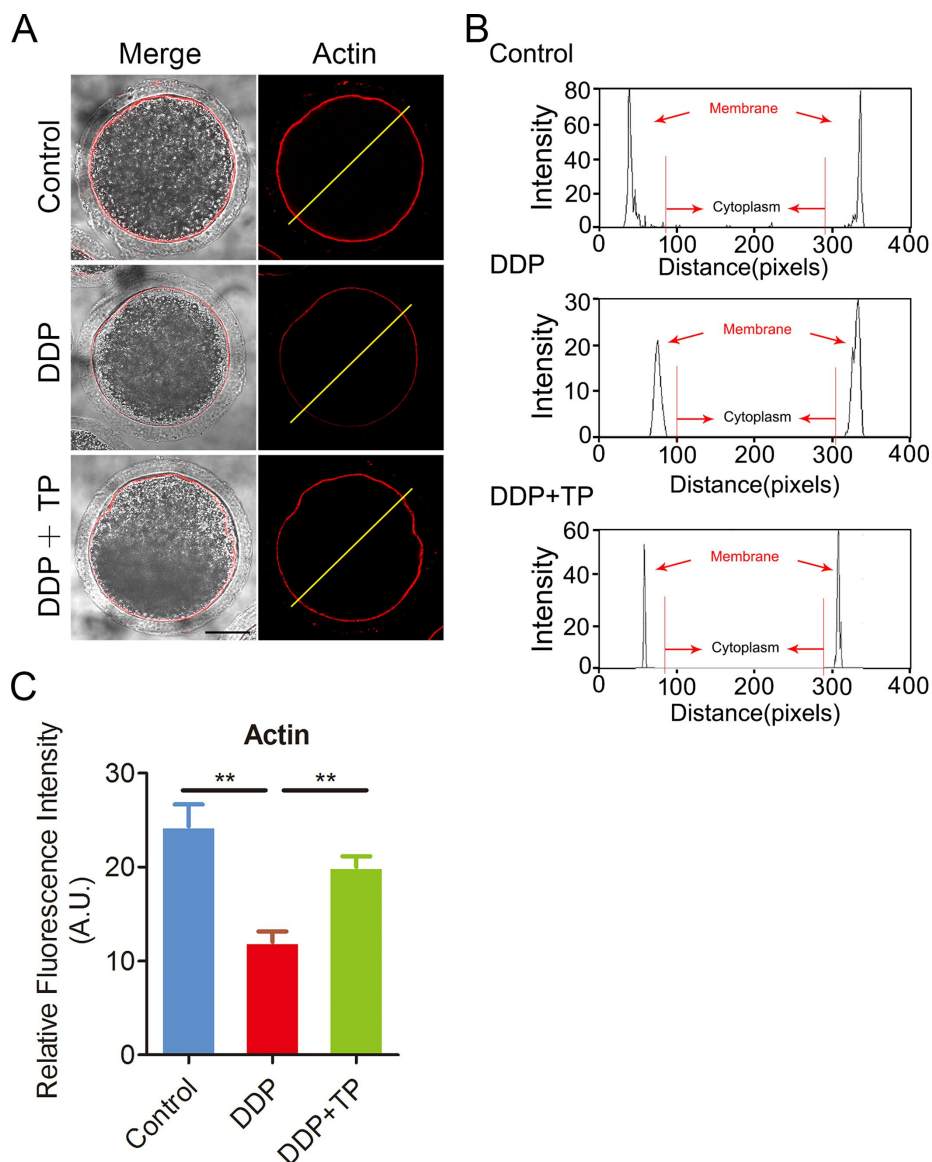


**Figure 4. Effects of TP on the actin polymerization in DDP-exposed porcine oocytes.** (A) Representative images of actin filaments in control, DDP-exposed and TP-supplemented oocytes. Scale bar, 30  $\mu\text{m}$ . (B) Right graphs show fluorescence intensity profiling of phalloidin in oocytes. Lines were drawn through the oocytes, and pixel intensities were quantified along the lines. (C) The fluorescence intensity of actin signals was measured in control, DDP-exposed and TP-supplemented oocytes. Data were presented as mean percentage (mean  $\pm$  SEM) of at least three independent experiments. \*\* $P < 0.01$ .

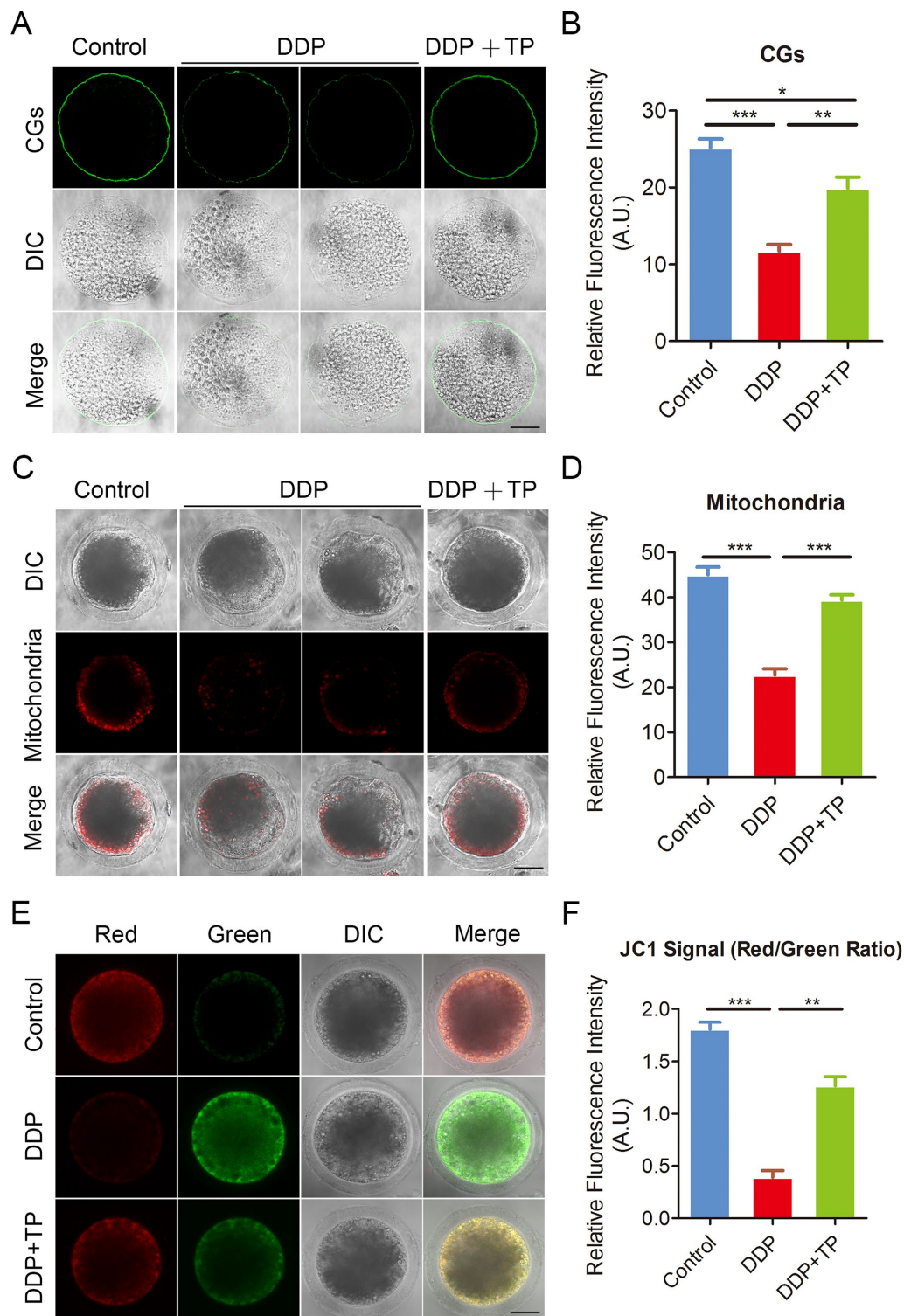


**Figure 5. Effects of TP on the distribution of CGs and mitochondria in DDP-exposed porcine oocytes.** (A) Representative images of CGs localization in control, DDP-exposed and TP-supplemented oocytes. Scale bar, 40  $\mu\text{m}$ . (B) The fluorescence intensity of cortical granules was measured in control, DDP-exposed and TP-supplemented oocytes. (C) Representative images of mitochondria in control, DDP-exposed and TP-supplemented oocytes. Scale bar, 35  $\mu\text{m}$ . (D) The immunofluorescence intensity of mitochondrion signals was recorded in control, DDP-exposed and TP-supplemented oocytes. (E) Mitochondrial membrane potential ( $\Delta\Psi\text{m}$ ) was detected by JC-1 in control, DDP-exposed and TP-supplemented oocytes (Red, high  $\Delta\Psi\text{m}$ ; Green, low  $\Delta\Psi\text{m}$ ). (F) The ratio of red and green fluorescence intensity was recorded in control, DDP-exposed and TP-supplemented oocytes. Data were presented as mean percentage (mean  $\pm$  SEM) of at least three independent experiments. \* $P < 0.05$ , \*\* $P < 0.01$ , \*\*\* $P < 0.001$ .

## TP suppresses oxidative stress, DNA damage and apoptosis induced by DDP exposure in porcine oocytes

DDP is known to induce oxidative stress in various cells to impair the cellular functions [40, 41], we then tested if the defects observed in DDP-exposed porcine oocytes were mediated by this mechanism. To verify this assumption, we compared the ROS levels between control and DDP-exposed oocytes by DCFH staining. The results showed that in control oocytes the signals were hardly detected (Figure 6A). However, DDP exposure remarkably increased the green signals in the cytoplasm of oocytes (Figure 6A). Consistently, the fluorescent intensity of ROS was significantly increased in DDP-exposed oocytes compared to controls ( $14.0 \pm 0.6$ ,  $n=29$  VS  $5.6 \pm 0.2$ ,  $n=29$ ,  $P < 0.001$ ; Figure 6B). Supplementation with TP effectively reduced the levels of ROS in DDP-exposed oocytes ( $7.9 \pm 0.5$ ,  $n=27$ ,  $P < 0.001$ ; Figure 6A, 6B).

Since the excessive oxidative stress always induces DNA damage and apoptosis [42, 43], we next assessed DNA damage and the early apoptosis in oocytes by  $\gamma$ -H2A.X and Annexin-V staining. The immunofluorescence results showed that the foci of  $\gamma$ -H2A.X were accumulated on the DNA in DDP-exposed oocytes instead of control oocytes, in agreement with the quantification data showing that the intensity of  $\gamma$ -H2A.X signals was remarkably elevated in DDP-exposed oocytes in comparison with the controls ( $26.4 \pm 1.1$ ,  $n=33$  VS  $10.1 \pm 0.4$ ,  $n=32$ ,  $P < 0.001$ ; Figure 7A,

7B). While treatment with TP markedly decreased the occurrence of DNA damage ( $15.2 \pm 0.8$ ,  $n=31$ ,  $P < 0.001$ ; Figure 7A, 7B). Also, we observed that the fluorescent signals of Annexin-V were rarely present in control oocytes, but clearly found on the plasma membrane of DDP-exposed oocytes (Figure 8A). Concordantly, the rate of apoptotic oocytes was dramatically higher in DDP-exposed group than that in controls ( $24.0 \pm 2.0$ ,  $n=36$  VS  $6.5 \pm 0.7$ ,  $n=38$ ,  $P < 0.01$ ; Figure 8A, 8B), but rescued in TP-supplemented group ( $11.8 \pm 0.9$ ,  $n=41$ ;  $P < 0.01$ ; Figure 8A, 8B).

## DISCUSSION

DDP, one of the most common chemotherapeutic drugs, is a DNA cross-linking agent widely used in the treatment of sarcomas and germ cell tumors. Its precise mechanism of action is not entirely clear, although it is known to intercalate with DNA strands causing crosslinking and adduct formation. DDP is categorized as a member of the intermediate gonadal risk group of drugs and has been reported to cause ovarian failure [6, 44]. However, the effects of DDP exposure on the oocyte quality have not yet defined.

To address this question, we investigated the critical biological events occurred during meiotic progression that drives the nuclear and cytoplasmic maturation of oocytes. Our findings revealed that oocytes exhibited a remarkably reduced proportion of polar body extrusion with impaired expansion of cumulus cells when treated with increasing concentrations of DDP, suggesting that

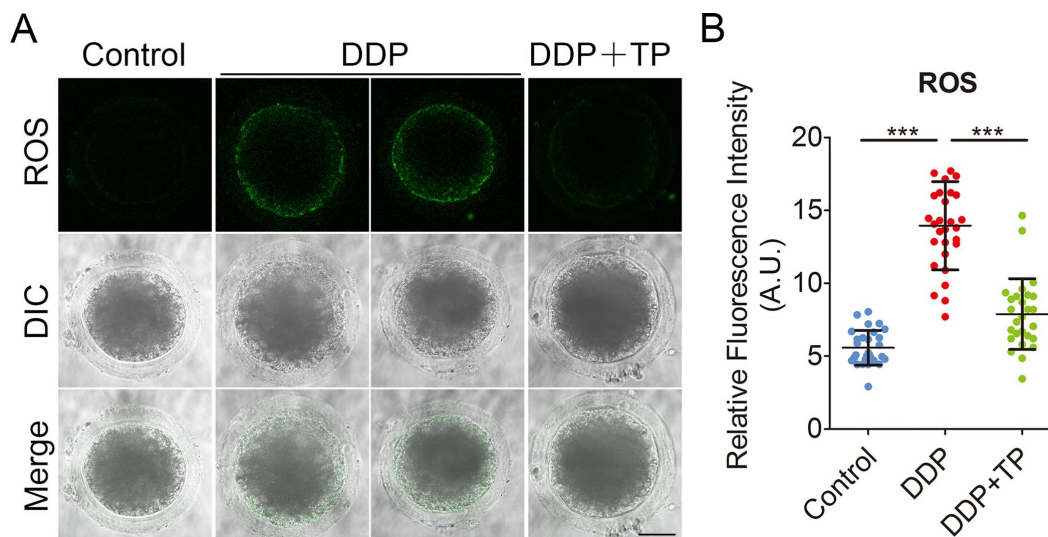


**Figure 6. Effects of TP on the ROS level in DDP-exposed porcine oocytes.** (A) Representative images of ROS levels in control, DDP-exposed and TP-supplemented oocytes. Scale bar, 35  $\mu$ m (B) The fluorescence intensity of ROS in control, DDP-exposed and TP-supplemented oocytes were measured by the confocal microscopy using identical settings and parameters. Data were presented as mean percentage (mean  $\pm$  SD) of at least three independent experiments. \*\*\* $P < 0.001$ .



DDP exposure perturbs the normal oocyte meiotic maturation. Further, the compromised nuclear maturation of oocytes was evidenced by the observations that spindle structure and chromosome alignment were severely disrupted in DDP-exposed oocytes. The abnormalities of spindle assembly prompted us to assess the microtubule dynamics by evaluating the acetylation level of tubulin, a posttranslational modification that occurs on Lys-40 of the  $\alpha$ -tubulin subunit to stabilize the microtubules in oocytes [32, 45]. Expectedly, our data illustrated that

DDP exposure decreased the acetylation level of  $\alpha$ -tubulin, indicating that the loss of microtubule stability might be one of the major causes leading to the disorganized spindle structure. Additionally, the dynamics of actin filament, another indispensable component of cytoskeleton, has been reported to play important roles in spindle positioning and meiotic progression during oocyte meiosis [46–48]. Our findings validated that the perturbed actin polymerization might be another major reason resulting in the oocyte meiotic failure when exposed to DDP.

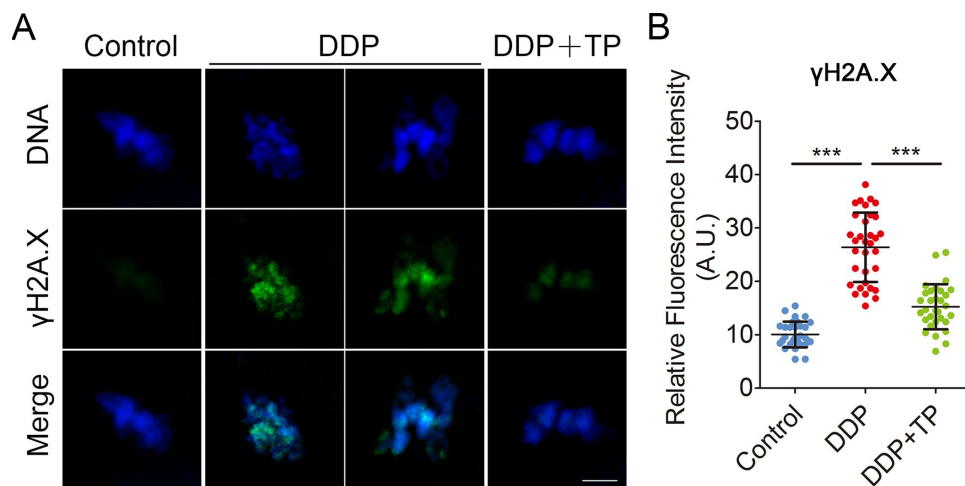


**Figure 7. Effects of TP on DNA damage in DDP-exposed porcine oocytes.** (A) Representative images of DNA damage in control, DDP-exposed and TP-supplemented groups. Scale bar, 5  $\mu$ m. (B) The fluorescence intensity of  $\gamma$ H2A.X signals was measured in control, DDP-exposed and TP-supplemented groups. Data in (B) were presented as mean percentage (mean  $\pm$  SD) of at least three independent experiments. \*\*\*P < 0.001.

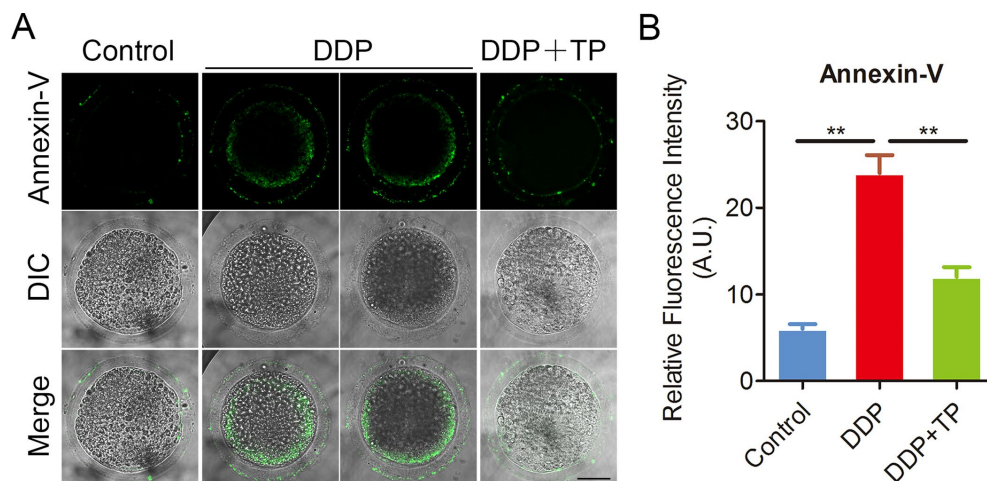


**Figure 8. Effects of TP on early apoptosis in DDP-exposed porcine oocytes.** (A) Representative images of apoptotic oocytes in control, DDP-exposed and TP-supplemented groups. Scale bar, 35  $\mu$ m. (B) The rate of early apoptosis was recorded in control, DDP-exposed and TP-supplemented oocytes. Data in (B) were presented as mean percentage (mean  $\pm$  SEM) of at least three independent experiments. \*\*P < 0.01.

Mitochondrion is a primary organelle that provides the source of ATP for oocyte development [49–51], and its integrity has been regarded as one of the key indexes of cytoplasmic maturation of oocytes. Our data found that the distribution of mitochondria was considerably impaired in oocytes exposed to DDP, suggesting that DDP exposure compromises the cytoplasmic maturation of oocytes via damaging the functionality of the mitochondria. Furthermore, another sign of oocyte cytoplasmic maturation is the proper distribution of cortical granules, a type of oocyte-specific vesicles that locate in the subcortical region of oocytes to exert functions in the prevention of polyspermy following fertilization [39]. We showed that the amount of cortical granules in the subcortex of DDP-exposed oocytes were significantly reduced, confirming the defective cytoplasmic maturation of oocytes as a result of DDP exposure.

Finally, we found that DDP-exposed porcine oocytes displayed a much higher level of ROS and the incidence of DNA damage as well as apoptosis, which might be cause for the DDP exposure-induced low quality of oocytes. More importantly, we documented that TP supplementation is able to, at least partially, recover all of the meiotic defects we observed in DDP-exposed oocytes via eliminating the excessive ROS, which in turn inhibits the accumulation of DNA damage and occurrence of apoptosis. These findings potentially provide an effective strategy to ameliorate the quality of oocytes from DDP-treated patients with cancer.

## MATERIALS AND METHODS

### Reagents

Mouse monoclonal anti- $\alpha$ -tubulin FITC antibody, anti-phalloidin-TRITC antibody, anti-acetyl- $\alpha$ -tubulin (Lys-40) antibody and lens culinaris agglutinin (LCA)-FITC were purchased from Sigma (St. Louis, MO, USA); FITC-conjugated goat anti-mouse IgG (H + L) and TRITC-conjugated goat anti-mouse IgG (H + L) were purchased from Zhongshan Golden Bridge Biotechnology Co., LTD (Beijing, China). DDP was purchased from Beijing Solarbio Science and Technology Co., LTD. (Beijing, China). TP was from Selleck Chemicals (Houston, TX, USA).

### Oocyte collection and *in vitro* maturation (IVM)

For *in vitro* maturation (IVM), ovaries were collected from prepubertal gilts at a local abattoir and transported to the laboratory in a 0.9% NaCl solution containing penicillin G (75 mg/ml) and streptomycin sulphate (50 mg/ml). Soon afterwards ovaries were washed twice with sterile phosphate-buffered saline (PBS), the Cumulus-

oocyte complexes (COCs) were subsequently aspirated from medium-sized follicles (3–6 mm in diameter) using a 20-gauge needle attached to a 20 ml disposable syringe. COCs surrounded by a compact cumulus mass with evenly granulated cytoplasm were washed three times with maturation medium, separated from the cellular debris, and then transferred to the maturation medium. The basic maturation medium was improved TCM-199 supplemented with 75  $\mu$ g/ml of penicillin, 50  $\mu$ g/ml of streptomycin, 0.5  $\mu$ g/ml of LH, 0.5  $\mu$ g/ml of FSH, 10 ng/ml of EGF and 0.57 mM cysteine. To prepare mature oocytes *in vitro*, a group of 30 COCs was transferred to 100  $\mu$ l of maturation medium and then covered with 100  $\mu$ l paraffin oil to culture at 38.5°C in a humidified atmosphere of 5% CO<sub>2</sub>.

### DDP and TP treatment

DDP was dissolved in DMF then in TCM-199 culture medium to a final concentration of 2,5,10 and 20  $\mu$ M. TP was dissolved in PBS and diluted with maturation medium to a final concentration of 10  $\mu$ M, 50  $\mu$ M and 250  $\mu$ M. It should be added to maturation medium immediately before use. The final concentrations of DMF in the culture medium were not more than 0.1%.

### Immunofluorescence staining and confocal microscopy

DOs were collected and fixed in 4% paraformaldehyde (PFA) in PBS for 30 min at room temperature. They were then washed three times in wash buffer, and were permeabilized in 1% Triton X-100 (in PBS) for 1 h at room temperature. After three further washes, they were blocked with blocking buffer (1% BSA-supplemented PBS) for 1 h at room temperature to suppress the non-specific binding of IgG. DOs were then incubated with primary antibodies overnight at 4°C, washed three more times, and incubated with secondary antibody for 1 h at room temperature. Finally, propidium iodide (PI) was used to stain nuclei for 10 min at room temperature. Samples were mounted on glass slides and examined with a confocal laser-scanning microscope (LSM 700 META; Zeiss, Germany).

### Immunoblotting analysis

A total of 120 porcine oocytes was collected and lysed in 4 $\times$  NuPAGE™ LDS sample buffer (ThermoFisher, USA) containing protease inhibitor, and then separated on 10% Bis-Tris precast gels and transferred onto polyvinylidene difluoride (PVDF) membranes. The blots were blocked in Tris buffered saline Tween 20 (TBST) containing 5% low fat dry milk for 1 h at room temperature and then incubated with anti-acetylated  $\alpha$ -tubulin antibody (1:1000) or anti-Gapdh (1:5000)

antibody overnight at 4°C. After washing in TBST, the blots were incubated with horseradish peroxidase (HRP)-conjugated secondary antibodies for 1 h at room temperature. Chemiluminescence was detected with ECL Plus (GE Healthcare, USA) and protein bands were visualized by Tanon-3900 (Tanon, China).

### Evaluation of mitochondrion distribution

Matured oocytes were stained for active mitochondria in the maturation medium containing 500 nM cell permeant MitoTracker Red CMXRos (ThermoFisher) for 30 min at 38.5°C in a dark environment and 5% CO<sub>2</sub> in air. After washing three times with maturation medium, oocytes were mounted on non-fluorescent glass slides and observed under the laser-scanning confocal microscope.

### Assessment of mitochondrial membrane potential

Mitochondrial membrane potential was evaluated using MitoProbe JC-1 Assay Kit (M34152, Thermo, USA). Briefly, oocytes were cultured in TCM-199 medium with 2 μM JC-1 for 30 min at 38.5°C, followed by washing with buffer for 10 min. Samples were immediately imaged in a glass bottom dish on the laser scanning confocal microscope. JC-1 dye exhibits potential-dependent accumulation in mitochondria, indicated by a fluorescence emission shift from green (~529 nm) to red (~590 nm). Thus, mitochondrial depolarization is indicated by a decrease in the red/green fluorescence intensity ratio. ImageJ software was used to quantify the intensity of fluorescence.

### Determination of ROS generation

To determine the levels of intracellular ROS production, denuded oocytes were incubated with the oxidation-sensitive fluorescent probe dichlorofluorescein (DCFH) for 30 min at 38.5°C in D-PBS that contained 10 μM DCFH diacetate (DCFHDA) (Beyotime Institute of Biotechnology, China). Then oocytes were washed three times in D-PBS containing 0.1% BSA, placed on glass slides and observed under the confocal microscope.

### Annexin-V staining

Denuded oocytes were stained with the Annexin-V staining kit (Vazyme, Nanjing, China) according to the manufacturer's instruction. After washing twice in PBS, the viable oocytes were stained for 30 min in the dark with 90 μl of binding buffer containing 10 μl of Annexin-V-FITC. Then oocytes were washed three times in D-PBS containing 0.1% BSA, placed on glass slides and observed under the confocal microscope.

### Statistical analysis

All percentages from at least three repeated experiments were expressed as mean ± SEM or mean ± SD, and the number of oocytes observed was labeled in parentheses as (n). Data were analyzed by one-way ANOVA or *t* test, which was provided by SPSS 16.0 statistical software (SPSS, Chicago, IL, USA). The level of significance was accepted as *P* < 0.05.

### CONFLICTS OF INTEREST

The authors have no conflicts of interest to disclose.

### FUNDING

This work was supported by the National Key Research and Development Program of China (2018YFC1003802), the Fundamental Research Funds for the Central Universities (KJYQ201901), the National Natural Science Foundation of China (31571545), and the Natural Science Foundation of Jiangsu Province (BK20161377).

### REFERENCES

1. Gómez-Ruiz S, Maksimović-Ivanić D, Mijatović S, Kaluđerović GN. On the discovery, biological effects, and use of Cisplatin and metallocenes in anticancer chemotherapy. *Bioinorg Chem Appl.* 2012; 2012:140284. <https://doi.org/10.1155/2012/140284> PMID:22844263
2. Ferreira JA, Peixoto A, Neves M, Gaiteiro C, Reis CA, Assaraf YG, Santos LL. Mechanisms of cisplatin resistance and targeting of cancer stem cells: adding glycosylation to the equation. *Drug Resist Updat.* 2016; 24:34–54. <https://doi.org/10.1016/j.drug.2015.11.003> PMID:26830314
3. Siddik ZH. Cisplatin: mode of cytotoxic action and molecular basis of resistance. *Oncogene.* 2003; 22:7265–79. <https://doi.org/10.1038/sj.onc.1206933> PMID:14576837
4. Arriagada R, Bergman B, Dunant A, Le Chevalier T, Pignon JP, Vansteenkiste J, and International Adjuvant Lung Cancer Trial Collaborative Group. Cisplatin-based adjuvant chemotherapy in patients with completely resected non-small-cell lung cancer. *N Engl J Med.* 2004; 350:351–60. <https://doi.org/10.1056/NEJMoa031644> PMID:14736927
5. McGuire WP, Hoskins WJ, Brady MF, Kucera PR, Partridge EE, Look KY, Clarke-Pearson DL, Davidson

- M. Cyclophosphamide and cisplatin compared with paclitaxel and cisplatin in patients with stage III and stage IV ovarian cancer. *N Engl J Med*. 1996; 334:1–6. <https://doi.org/10.1056/NEJM199601043340101> PMID:7494563
6. Yeh J, Kim B, Liang YJ, Peresie J. Müllerian inhibiting substance as a novel biomarker of cisplatin-induced ovarian damage. *Biochem Biophys Res Commun*. 2006; 348:337–44. <https://doi.org/10.1016/j.bbrc.2006.06.195> PMID:16875679
  7. Macciò A, Madeddu C. Cisplatin : an old drug with a newfound efficacy — from mechanisms of action to cytotoxicity. *Expert Opin Pharmacother*. 2013; 14:1839–57. <https://doi.org/10.1517/14656566.2013.813934> PMID:23876094
  8. Roos WP, Kaina B. DNA damage-induced cell death by apoptosis. *Trends Mol Med*. 2006; 12:440–50. <https://doi.org/10.1016/j.molmed.2006.07.007> PMID:16899408
  9. Casares C, Ramírez-Camacho R, Trinidad A, Roldán A, Jorge E, García-Berrocal JR. Reactive oxygen species in apoptosis induced by cisplatin: review of physiopathological mechanisms in animal models. *Eur Arch Otorhinolaryngol*. 2012; 269:2455–59. <https://doi.org/10.1007/s00405-012-2029-0> PMID:22584749
  10. Karasawa T, Steyger PS. An integrated view of cisplatin-induced nephrotoxicity and ototoxicity. *Toxicol Lett*. 2015; 237:219–27. <https://doi.org/10.1016/j.toxlet.2015.06.012> PMID:26101797
  11. Meistrich ML. Male gonadal toxicity. *Pediatr Blood Cancer*. 2009; 53:261–66. <https://doi.org/10.1002/pbc.22004> PMID:19326418
  12. Chang EM, Lim E, Yoon S, Jeong K, Bae S, Lee DR, Yoon TK, Choi Y, Lee WS. Cisplatin Induces Overactivation of the Dormant Primordial Follicle through PTEN/AKT/FOXO3a Pathway which Leads to Loss of Ovarian Reserve in Mice. *PLoS One*. 2015; 10:e0144245. <https://doi.org/10.1371/journal.pone.0144245> PMID:26656301
  13. Rossi V, Lispi M, Longobardi S, Mattei M, Di Rella F, Salustri A, De Felici M, Klinger FG. LH prevents cisplatin-induced apoptosis in oocytes and preserves female fertility in mouse. *Cell Death Differ*. 2017; 24:72–82. <https://doi.org/10.1038/cdd.2016.97> PMID:27689876
  14. Suh EK, Yang A, Kettenbach A, Bamberger C, Michaelis AH, Zhu Z, Elvin JA, Bronson RT, Crum CP, McKeon F. p63 protects the female germ line during meiotic arrest. *Nature*. 2006; 444:624–28. <https://doi.org/10.1038/nature05337> PMID:17122775
  15. Mukhtar H, Ahmad N. Tea polyphenols: prevention of cancer and optimizing health. *Am J Clin Nutr*. 2000 (Suppl); 71:1698S–702S. <https://doi.org/10.1093/ajcn/71.6.1698S> PMID:10837321
  16. Frei B, Higdon JV. Antioxidant activity of tea polyphenols in vivo: evidence from animal studies. *J Nutr*. 2003; 133:3275S–84S. <https://doi.org/10.1093/jn/133.10.3275S> PMID:14519826
  17. Glei M, Pool-Zobel BL. The main catechin of green tea, (-)-epigallocatechin-3-gallate (EGCG), reduces bleomycin-induced DNA damage in human leucocytes. *Toxicol In Vitro*. 2006; 20:295–300. <https://doi.org/10.1016/j.tiv.2005.08.002> PMID:16188420
  18. Yen GC, Ju JW, Wu CH. Modulation of tea and tea polyphenols on benzo(a)pyrene-induced DNA damage in Chang liver cells. *Free Radic Res*. 2004; 38:193–200. <https://doi.org/10.1080/10715760310001638001> PMID:15104213
  19. Jiang T, Glickman BW, de Boer JG. Protective effect of green tea against benzo[a]pyrene-induced mutations in the liver of Big Blue transgenic mice. *Mutat Res*. 2001; 480-481:147–51. [https://doi.org/10.1016/S0027-5107\(01\)00178-6](https://doi.org/10.1016/S0027-5107(01)00178-6) PMID:11506808
  20. Kaur S, Greaves P, Cooke DN, Edwards R, Steward WP, Gescher AJ, Marczylo TH. Breast cancer prevention by green tea catechins and black tea theaflavins in the C3(1) SV40 T,t antigen transgenic mouse model is accompanied by increased apoptosis and a decrease in oxidative DNA adducts. *J Agric Food Chem*. 2007; 55:3378–85. <https://doi.org/10.1021/jf0633342> PMID:17407311
  21. Ding J, Wang H, Wu ZB, Zhao J, Zhang S, Li W. Protection of murine spermatogenesis against ionizing radiation-induced testicular injury by a green tea polyphenol. *Biol Reprod*. 2015; 92:6. <https://doi.org/10.1095/biolreprod.114.122333> PMID:25395675
  22. Wang ZG, Yu SD, Xu ZR. Improvement in bovine embryo production in vitro by treatment with green tea polyphenols during in vitro maturation of oocytes. *Anim Reprod Sci*. 2007; 100:22–31. <https://doi.org/10.1016/j.anireprosci.2006.06.014> PMID:16870363

23. Wang ZG, Yu SD, Xu ZR. Effect of supplementation of green tea polyphenols on the developmental competence of bovine oocytes in vitro. *Braz J Med Biol Res.* 2007; 40:1079–85.  
<https://doi.org/10.1590/S0100-879X2007000800008>  
PMID:[17665044](https://pubmed.ncbi.nlm.nih.gov/17665044/)
24. Luo LL, Huang J, Fu YC, Xu JJ, Qian YS. Effects of tea polyphenols on ovarian development in rats. *J Endocrinol Invest.* 2008; 31:1110–18.  
<https://doi.org/10.1007/BF03345661> PMID:[19246979](https://pubmed.ncbi.nlm.nih.gov/19246979/)
25. Wang Z, Fu C, Yu S. Green tea polyphenols added to IVM and IVC media affect transcript abundance, apoptosis, and pregnancy rates in bovine embryos. *Theriogenology.* 2013; 79:186–92.  
<https://doi.org/10.1016/j.theriogenology.2012.10.002>  
PMID:[23122606](https://pubmed.ncbi.nlm.nih.gov/23122606/)
26. Schatten H, Sun QY. Centrosome dynamics during mammalian oocyte maturation with a focus on meiotic spindle formation. *Mol Reprod Dev.* 2011; 78:757–68.  
<https://doi.org/10.1002/mrd.21380> PMID:[21887720](https://pubmed.ncbi.nlm.nih.gov/21887720/)
27. Kobayashi E, Hishikawa S, Teratani T, Lefor AT. The pig as a model for translational research: overview of porcine animal models at Jichi Medical University. *Transplant Res.* 2012; 1:8.  
<https://doi.org/10.1186/2047-1440-1-8>  
PMID: [23369409](https://pubmed.ncbi.nlm.nih.gov/23369409/)
28. Zhang L, Hou X, Ma R, Moley K, Schedl T, Wang Q. Sirt2 functions in spindle organization and chromosome alignment in mouse oocyte meiosis. *FASEB J.* 2014; 28:1435–45.  
<https://doi.org/10.1096/fj.13-244111>  
PMID:[24334550](https://pubmed.ncbi.nlm.nih.gov/24334550/)
29. Zhang M, Miao Y, Chen Q, Cai M, Dong W, Dai X, Lu Y, Zhou C, Cui Z, Xiong B. BaP exposure causes oocyte meiotic arrest and fertilization failure to weaken female fertility. *FASEB J.* 2018; 32:342–352.  
<https://doi.org/10.1096/fj.201700514R>  
PMID:[28904021](https://pubmed.ncbi.nlm.nih.gov/28904021/)
30. Montagnac G, Meas-Yedid V, Irodelles M, Castro-Castro A, Franco M, Shida T, Nachury MV, Benmerah A, Olivo-Marin JC, Chavier P.  $\alpha$ TAT1 catalyses microtubule acetylation at clathrin-coated pits. *Nature.* 2013; 502:567–70.  
<https://doi.org/10.1038/nature12571>  
PMID:[24097348](https://pubmed.ncbi.nlm.nih.gov/24097348/)
31. Xu Z, Schaedel L, Portran D, Aguilar A, Gaillard J, Marinkovich MP, Théry M, Nachury MV. Microtubules acquire resistance from mechanical breakage through intraluminal acetylation. *Science.* 2017; 356:328–32.  
<https://doi.org/10.1126/science.aai8764>  
PMID:[28428427](https://pubmed.ncbi.nlm.nih.gov/28428427/)
32. Lu Y, Li S, Cui Z, Dai X, Zhang M, Miao Y, Zhou C, Ou X, Xiong B. The cohesion establishment factor Esco1 acetylates  $\alpha$ -tubulin to ensure proper spindle assembly in oocyte meiosis. *Nucleic Acids Res.* 2018; 46:2335–46.  
<https://doi.org/10.1093/nar/gky001>  
PMID:[29361031](https://pubmed.ncbi.nlm.nih.gov/29361031/)
33. Miao Y, Zhou C, Cui Z, Zhang M, Shiyang X, Lu Y, Xiong B. Postovulatory aging causes the deterioration of porcine oocytes via induction of oxidative stress. *FASEB J.* 2018; 32:1328–1337.  
<https://doi.org/10.1096/fj.201700908R>  
PMID:[29109171](https://pubmed.ncbi.nlm.nih.gov/29109171/)
34. Azoury J, Lee KW, Georget V, Rassiner P, Leader B, Verlhac MH. Spindle positioning in mouse oocytes relies on a dynamic meshwork of actin filaments. *Curr Biol.* 2008; 18:1514–19.  
<https://doi.org/10.1016/j.cub.2008.08.044>  
PMID:[18848445](https://pubmed.ncbi.nlm.nih.gov/18848445/)
35. Pfender S, Kuznetsov V, Pleiser S, Kerkhoff E, Schuh M. Spire-type actin nucleators cooperate with Formin-2 to drive asymmetric oocyte division. *Curr Biol.* 2011; 21:955–60.  
<https://doi.org/10.1016/j.cub.2011.04.029>  
PMID:[21620703](https://pubmed.ncbi.nlm.nih.gov/21620703/)
36. Duan X, Sun SC. Actin cytoskeleton dynamics in mammalian oocyte meiosis. *Biol Reprod.* 2019; 100:15–24.  
<https://doi.org/10.1093/biolre/iory163>  
PMID:[30010726](https://pubmed.ncbi.nlm.nih.gov/30010726/)
37. Ducibella T, Anderson E, Albertini DF, Aalberg J, Rangarajan S. Quantitative studies of changes in cortical granule number and distribution in the mouse oocyte during meiotic maturation. *Dev Biol.* 1988; 130:184–97.  
[https://doi.org/10.1016/0012-1606\(88\)90425-3](https://doi.org/10.1016/0012-1606(88)90425-3)  
PMID:[3141231](https://pubmed.ncbi.nlm.nih.gov/3141231/)
38. Sun QY, Wu GM, Lai L, Park KW, Cabot R, Cheong HT, Day BN, Prather RS, Schatten H. Translocation of active mitochondria during pig oocyte maturation, fertilization and early embryo development in vitro. *Reproduction.* 2001; 122:155–63.  
<https://doi.org/10.1530/rep.0.1220155>  
PMID:[11425340](https://pubmed.ncbi.nlm.nih.gov/11425340/)
39. Burkart AD, Xiong B, Baibakov B, Jiménez-Movilla M, Dean J. Ovastacin, a cortical granule protease, cleaves ZP2 in the zona pellucida to prevent polyspermy. *J Cell Biol.* 2012; 197:37–44.  
<https://doi.org/10.1083/jcb.201112094>  
PMID:[22472438](https://pubmed.ncbi.nlm.nih.gov/22472438/)
40. Martins NM, Santos NA, Curti C, Bianchi ML, Santos AC. Cisplatin induces mitochondrial oxidative stress

- with resultant energetic metabolism impairment, membrane rigidification and apoptosis in rat liver. *J Appl Toxicol*. 2008; 28:337–44.  
<https://doi.org/10.1002/jat.1284> PMID:17604343
41. Santos NA, Catão CS, Martins NM, Curti C, Bianchi ML, Santos AC. Cisplatin-induced nephrotoxicity is associated with oxidative stress, redox state unbalance, impairment of energetic metabolism and apoptosis in rat kidney mitochondria. *Arch Toxicol*. 2007; 81:495–504.  
<https://doi.org/10.1007/s00204-006-0173-2> PMID:17216432
42. Ozben T. Oxidative stress and apoptosis: impact on cancer therapy. *J Pharm Sci*. 2007; 96:2181–96.  
<https://doi.org/10.1002/jps.20874> PMID:17593552
43. Ratan RR, Murphy TH, Baraban JM. Macromolecular synthesis inhibitors prevent oxidative stress-induced apoptosis in embryonic cortical neurons by shunting cysteine from protein synthesis to glutathione. *J Neurosci*. 1994; 14:4385–92.  
<https://doi.org/10.1523/JNEUROSCI.14-07-04385.1994> PMID:8027786
44. Blumenfeld Z. Chemotherapy and fertility. *Best Pract Res Clin Obstet Gynaecol*. 2012; 26:379–90.  
<https://doi.org/10.1016/j.bpobgyn.2011.11.008> PMID:22281514
45. Janke C, Montagnac G. Causes and Consequences of Microtubule Acetylation. *Curr Biol*. 2017; 27:R1287–92.  
<https://doi.org/10.1016/j.cub.2017.10.044> PMID:29207274
46. Zhang J, Ma R, Li L, Wang L, Hou X, Han L, Ge J, Li M, Wang Q. Intersectin 2 controls actin cap formation and meiotic division in mouse oocytes through the Cdc42 pathway. *FASEB J*. 2017; 31:4277–4285.  
<https://doi.org/10.1096/fj.201700179R> PMID:28626024
47. Wang QC, Liu J, Wang ZB, Zhang Y, Duan X, Cui XS, Kim NH, Sun SC. Dynamin 2 regulates actin-mediated spindle migration in mouse oocytes. *Biol Cell*. 2014; 106:193–202.  
<https://doi.org/10.1111/boc.201400007> PMID:24735075
48. Wang H, Guo J, Lin Z, Namgoong S, Oh JS, Kim NH. Filamin A is required for spindle migration and asymmetric division in mouse oocytes. *FASEB J*. 2017; 31:3677–88.  
<https://doi.org/10.1096/fj.201700056R> PMID:28487281
49. Perez GI, Trbovich AM, Gosden RG, Tilly JL. Mitochondria and the death of oocytes. *Nature*. 2000; 403:500–01.  
<https://doi.org/10.1038/35000651> PMID:10676949
50. Dumollard R, Duchen M, Carroll J. The role of mitochondrial function in the oocyte and embryo. *Curr Top Dev Biol*. 2007; 77:21–49.  
[https://doi.org/10.1016/S0070-2153\(06\)77002-8](https://doi.org/10.1016/S0070-2153(06)77002-8) PMID:17222699
51. Niu YJ, Nie ZW, Shin KT, Zhou W, Cui XS. PINK1 regulates mitochondrial morphology *via* promoting mitochondrial fission in porcine preimplantation embryos. *FASEB J*. 2019; 33:7882–95.  
<https://doi.org/10.1096/fj.201802473R> PMID:30897005